Electronic Supplementary Material (ESI) for Nanoscale.
This journal is © The Royal Society of Chemistry 2016

Supplementary Information

Ultrasound-Mediated Modulation of the Emission of Gold Nanodots

Yu-Ting Tseng,[‡a] Rochelle Cherng,[‡b] Zhiqin Yuan,[c] Chien-Wei Wu,[a] Huan-Tsung Chang,[*a] and Chih-Ching Huang[*bde]

[a]Department of Chemistry, National Taiwan University, Taipei, 10617, Taiwan

[b]Department of Bioscience and Biotechnology, National Taiwan Ocean University, Keelung, 20224, Taiwan

[c]State Key Laboratory of Chemical Resource Engineering, Beijing University of Chemical Technology, Beijing, 100029, China

[d]Center of Excellence for the Oceans, National Taiwan Ocean University, Keelung, 20224, Taiwan

[e]School of Pharmacy, College of Pharmacy, Kaohsiung Medical University, Kaohsiung, 80708, Taiwan

[‡]These authors contributed equally to the work

Correspondence: Huan-Tsung Chang, Department of Chemistry, National Taiwan University, 1, Section 4, Roosevelt Road, Taipei 10617, Taiwan; tel. and fax: 011-886-2-3366-1171; e-mail: changht@ntu.edu.tw; Chih-Ching Huang, Department of Bioscience and Biotechnology, National Taiwan Ocean University, 2, Beining Road, Keelung 20224, Taiwan; tel.: 011-886-2-2462-2192 ext5517; fax: 011-886-2-2462-2320; e-mail: huanging@ntou.edu.tw

EXPERIMENTAL DETAILS

Synthesis and Characterizations of Au NPs. The gold nanoparticles (Au NPs) were synthesized through THPC-mediated reduction of $HAuCl_4 \cdot 3H_2O$, according to a slight modification of a reported procedure.[1] An aqueous solution (46 mL) was prepared containing 1.0 M NaOH and 80% THPC (13.5 μL). Next, 1% $HAuCl_4$ (1.5 mL) was added in one portion to the THPC solution under constant stirring. After stirring for 10 s, the color changed to brown, indicating the formation of the THPC–Au NPs. The solution was stored at room temperature for 5 min prior to use. The average size of the as-prepared Au NPs, determined through transmission electron microscopy (TEM; Tecnai 20 G2 S-Twin TEM, Philips/FEI, Hillsboro, Oregon), was 2.9 (± 0.5) nm. The particle concentration of the as-prepared Au NP solution was 2 μM, determined using the equation ($n = 3m/4\pi r^3 s$), assuming the presence of ideal spherical particles, where n is the number of gold particles per milliliter, m is the molar mass of gold in the substance (g/mL), r is the particle radius (cm), and s is the specific gravity of colloidal gold (19.3 g/cm^3). The values of m and r were determined using inductively coupled plasma mass spectroscopy (ICP-MS) and TEM, respectively. This formula gives the number of Au NPs per milliliter. This concentration was then converted into the number of gold particles per liter and divided by Avogadro's number (6.023×10^{23}) to give the final molar concentration of Au NPs.

Characterization of Photoluminescent Au NDs. UV–Vis absorption and PL spectra of the Au NDs were recorded using a Synergy 4 multimode monochromatic microplate spectrophotometer (Biotek Instruments, Winooski, VT, USA). QYs were determined by comparison with that of quinine (QY: 53%; in 0.1 M H_2SO_4). TEM measurements were conducted using a Tecnai 20 G2 S-Twin transmission electron microscope operating at 200 kV. Au NDs (50 nM, 50 μL) were deposited onto a TEM grid with a thin layer of carbon. X-ray photoelectron spectroscopy (XPS) was performed using an ES-CALAB 250 spectrometer (VG Scientific, East Grinstead, UK) with Al Kα X-rays as the source for excitation. Binding energies were corrected using the C 1s peak at 284.6 eV as a standard. The samples for XPS measurements were prepared by depositing drops of the Au NDs solution (1.0 μM, 100 μL) onto Si substrates and then evaporating the solvent at ambient temperature and pressure. The PL lifetimes of the Au NDs were recorded using a photo-counting PicoHarp 300 system (PicoPicoQuant, Berlin, Germany) and a diode laser emitting at 375 nm (FluoTime 300) as the light source.

Prior to conducting laser desorption/ionization mass spectrometry (LDI-MS), the as-prepared Au ND solutions (0.5 mL) were centrifuged at 18,000 *g* for 30 min. After removal of the supernatant solution, the precipitate was re-suspended in water and then subjected to three centrifugation/wash cycles to remove most of the free ligands. LDI-MS analyses of purified 11-MUTAB–Au NDs were performed in the reflectron positive-ion mode using an AutoflexIII LDI time-of-flight (TOF) mass spectrometer (Bruker Daltonics, Bremen, Germany). The samples were irradiated using pulsed laser irradiation (355-nm Nd:YAG, 100 Hz; pulse width: 6 ns). A total of 1000 pulsed laser shots (laser density: 6.37×10^4 W cm^{-2}) were applied to five random positions on the LDI target.

Quantitation of surface 11-MUTA or 11-MUA ligands on the Au NDs was accomplished by using a ESI-Q-TOF MS (Waters SYNAPT G2 HDMS, Waters Corp., Milford, MA, USA). The purified Au NDs (100 nM; 1.0 mL) were etched with 20 mM NaCN. A 5.0 μL aliquot of the etching sample solution was mixed with 5.0 μL of 50% ethanol solution, and analyzed by ESI-Q-TOF MS. Each of the mixtures were injected into a 180 μm (inner diameter) × 2.0 cm capillary trap column. The ESI-Q-TOF MS was operated with a spray voltage of 3.0 kV. NanoLockSpray source was used for accurate mass measurement, and the lock mass channel was sampled every 30 s. Data acquisition was operated in data direct analysis (DDA) mode. The mode included one full MS scan (*m/z* 100–1000 for 1.0 s) and three sequential MS/MS scans (m/z 100–1990, 1.5 s for each scan) on the three most intense ions present in the full scan mass spectrum. Each sample was analyzed in triplicate.

Reference:

(1) D. G. Duff andA. Baiker, A new hydrosol of gold clusters. 1. formation and particle size variation. *Langmuir* 1993, **9**, 2301–2309.

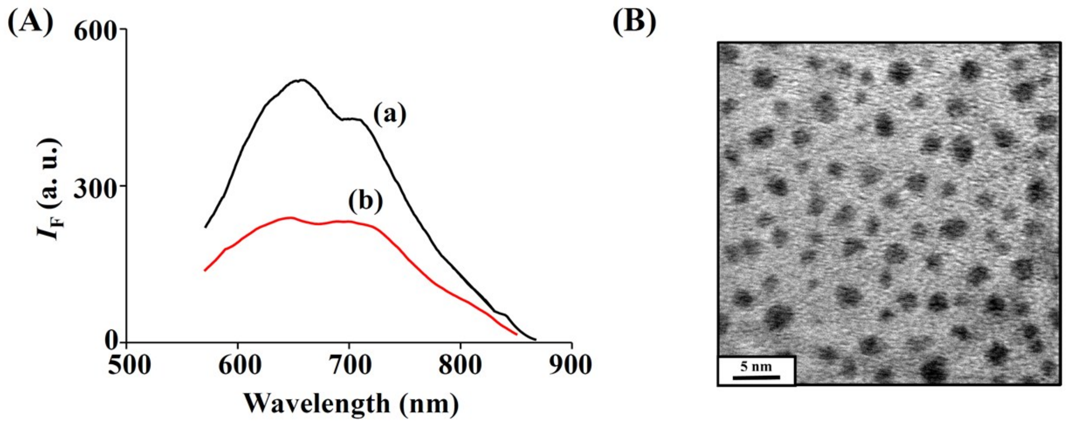

Fig. S1. PL emission spectra of 11-MUTAB–Au NDs prepared under (a) in air atmosphere and (b) N_2-saturated conditions (purging with 99.999% N_2; O_2<1 ppm). (B) TEM image of 11-MUTAB–Au NDs prepared in N_2-saturated conditions. Other conditions were the same as those described in Fig. 1.

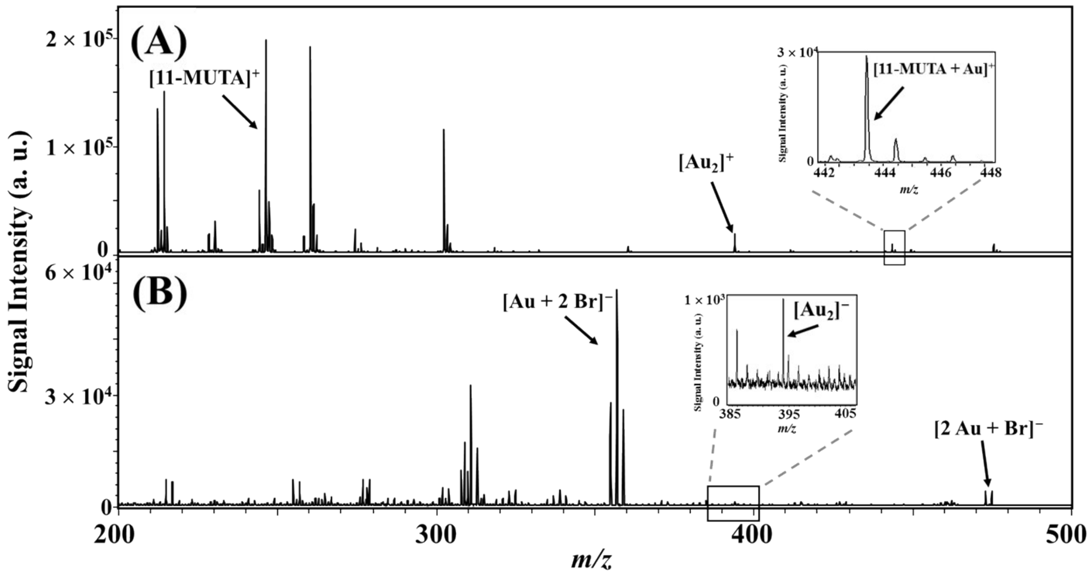

Fig. S2. LDI-TOF mass spectra of purified 11-MUTAB–Au NDs, recorded in (A) positive and (B) negative modes. Signals at *m*/*z* 246.73, 393.83, and 443.19 in (A) are assigned to [11-MUTA]$^+$, [Au_2]$^+$, and [11-MUTA + Au]$^+$ ions, respectively. Signals at *m*/*z* 356.80, 393.83, and 472.85 in (B) are assigned to [Au + 2Br]$^-$, [Au_2]$^-$, and [2Au + Br]$^-$ ions, respectively. A total of 1000 pulsed laser shots were applied to accumulate the signals from five LDI target positions under a laser power density of 6.37×10^4 W cm^{-2}. Signal intensities are plotted in arbitrary units (a. u.).

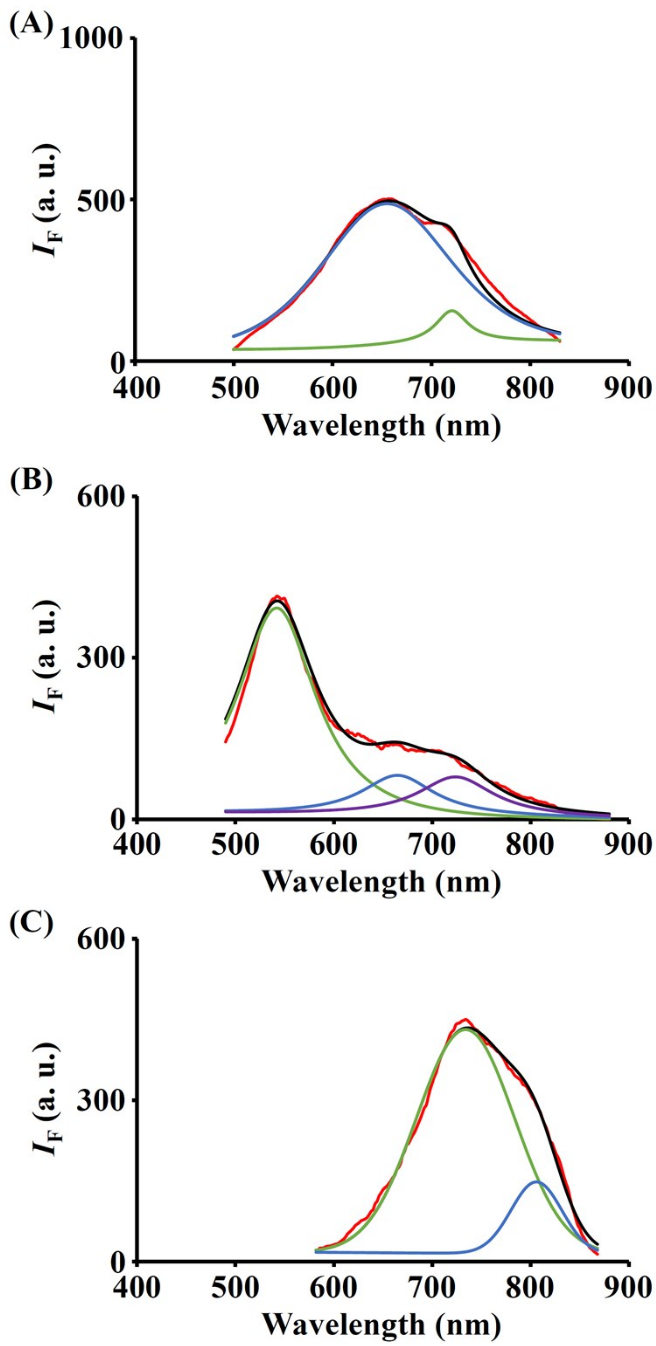

Fig. S3. Deconvoluted PL spectra (green, blue and purple curves) of (A) 11-MUTAB–Au NDs, (B) 11-MUTAB–Au $NDs_{0.5h/20w}$, and (C) 11-MUTAB–Au $NDs_{5.0h/20w}$. The total spectrum (sum of the deconvoluted PL spectra) were given in black curves. Other conditions were the same as those described in Fig. 1.

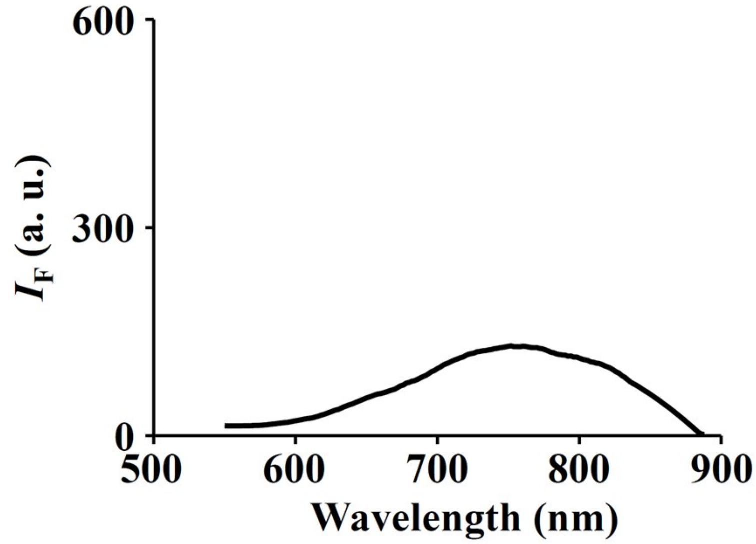

Fig. S4. PL spectra of mixtures of 11-MUTAB (1.0 mM) and $HAuCl_4$ (0.8 mM) in sodium tetraborate buffer (20 mM, pH 9.2). Excitation wavelength: 365 nm. Other conditions were the same as those described in Fig. 1.

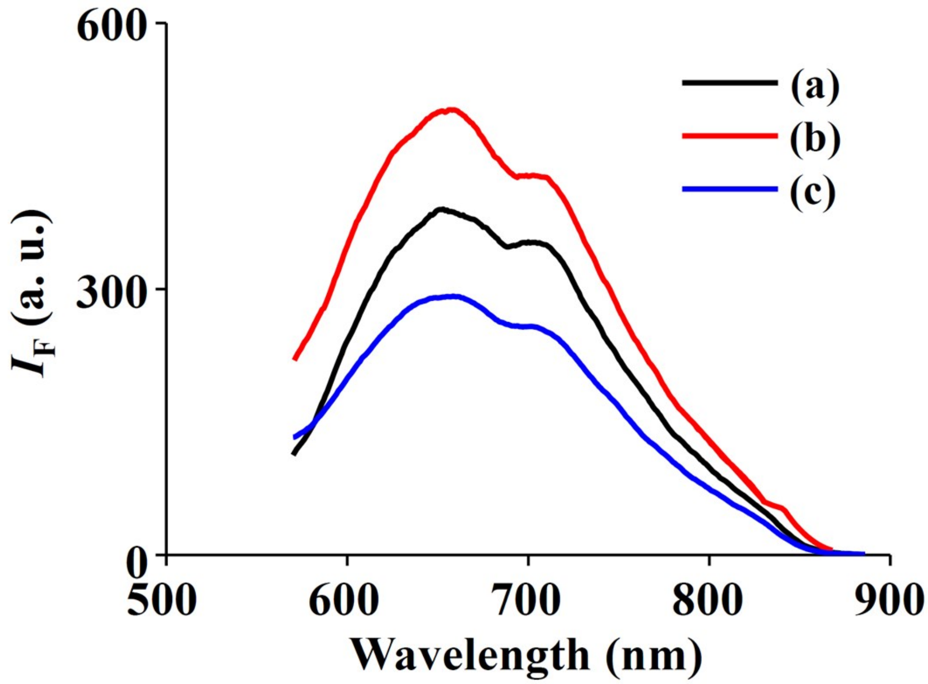

Fig. S5. PL emission spectra of 11-MUTAB–Au NDs at excitation wavelengths of (a) 345 nm, (b) 365 nm, and (c) 385 nm. Other conditions were the same as those described in Fig. 1.

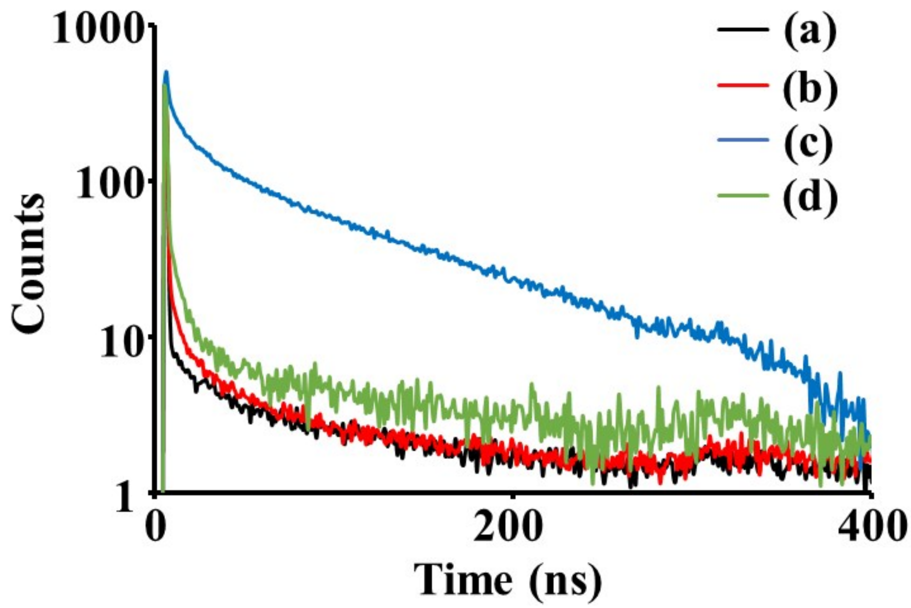

Fig. S6. PL lifetimes, after excitation at 375 nm, of (a) 11-MUTAB–Au NDs, (b) 11-MUTAB–Au NDs$_{0.5h/20w}$, (c) 11-MUTAB–Au NDs$_{2.0h/20w}$, and (d) 11-MUTAB–Au NDs$_{5.0h/20w}$ in sodium tetraborate buffer (20 mM, pH 9.2). The PL decay was fitted to a biexponential function. The PL emissions are collected at 670 nm, 540 m, 540 nm, and 810 nm for (a), (b), (c), and (d), respectively. Other conditions were the same as those described in Fig. 1.

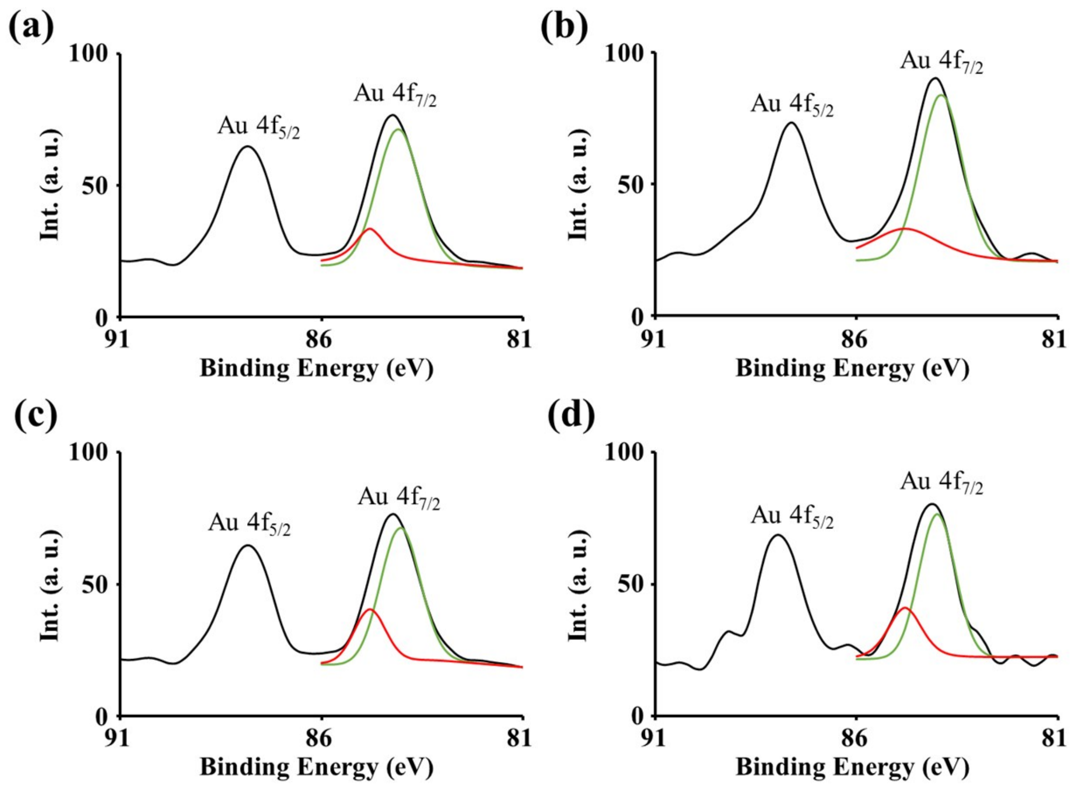

Fig. S7. XPS spectra of (a) 11-MUTAB–Au NDs, (b) 11-MUTAB–Au NDs$_{0.5h/20w}$, (c) 11-MUTAB–Au NDs$_{2.0h/20w}$, and (d) 11-MUTAB–Au NDs$_{5.0h/20w}$. The broad peaks (Au 4f$_{7/2}$) were deconvoluted into two distinct components (green and red lines) centered at binding energies of 84.1 and 84.8 eV, assigned to Au(0) and Au(I) species, respectively. Other conditions were the same as those described in Fig. 1.

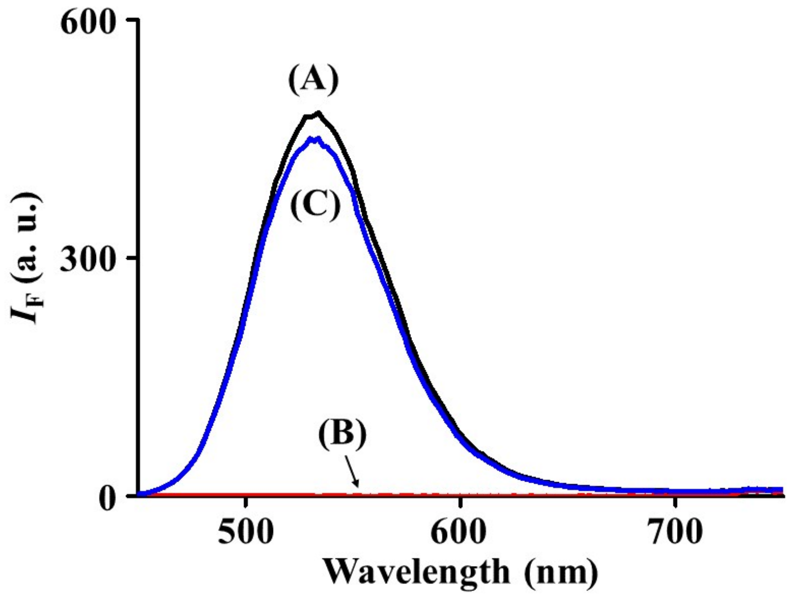

Fig. S8. PL emission spectra of (A) 11-MUTAB–Au NDs$_{2.0h/20w}$ (100 nM), (B) discarded solution after purification by centrifugal filtration (10,000 g; cutoff 10 kDa), and (C) resuspended 11-MUTAB–Au NDs$_{2.0h/20w}$ in 20 mM sodium tetraborate solution (pH 9.2). Excitation wavelength: 365 nm. Other conditions were the same as those described in Fig. 1.

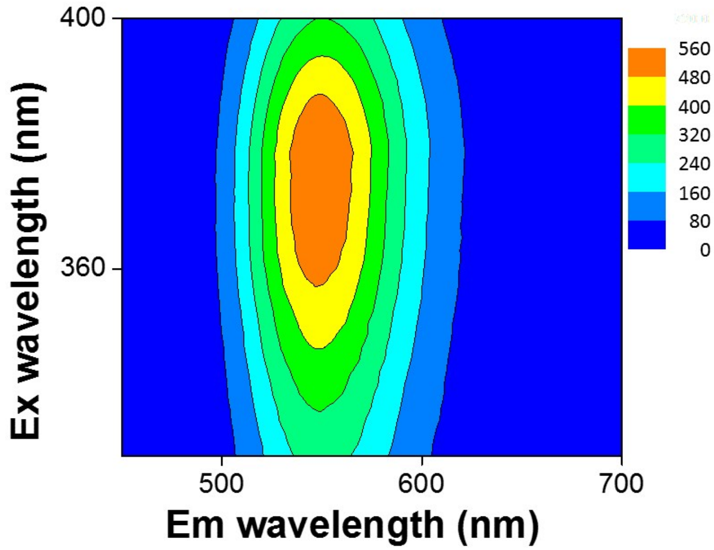

Fig. S9. Excitation/emission contour map of 11-MUTAB–Au $NDs_{2.0h/20w}$.

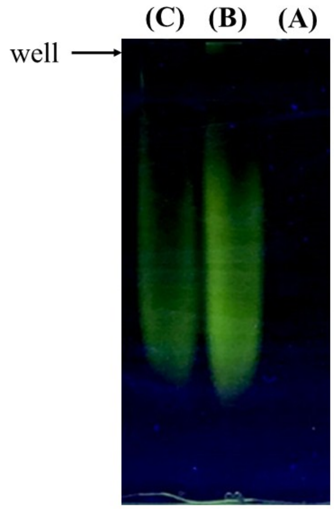

Fig. S10. Gel electrophoresis of 11-MUTAB–Au NDs$_{2.0h/20w}$ in native PAGE (4%) containing 192 mM glycine and 25 mM tris(hydroxymethylamine) buffer at a constant voltage mode (150 V). (A) 20 mM sodium tetraborate buffer solution as control. The concentration of 11-MUTAB–Au NDs$_{2.0h/20w}$ in (B) and (C) are 10 μM and 5 μM, respectively.

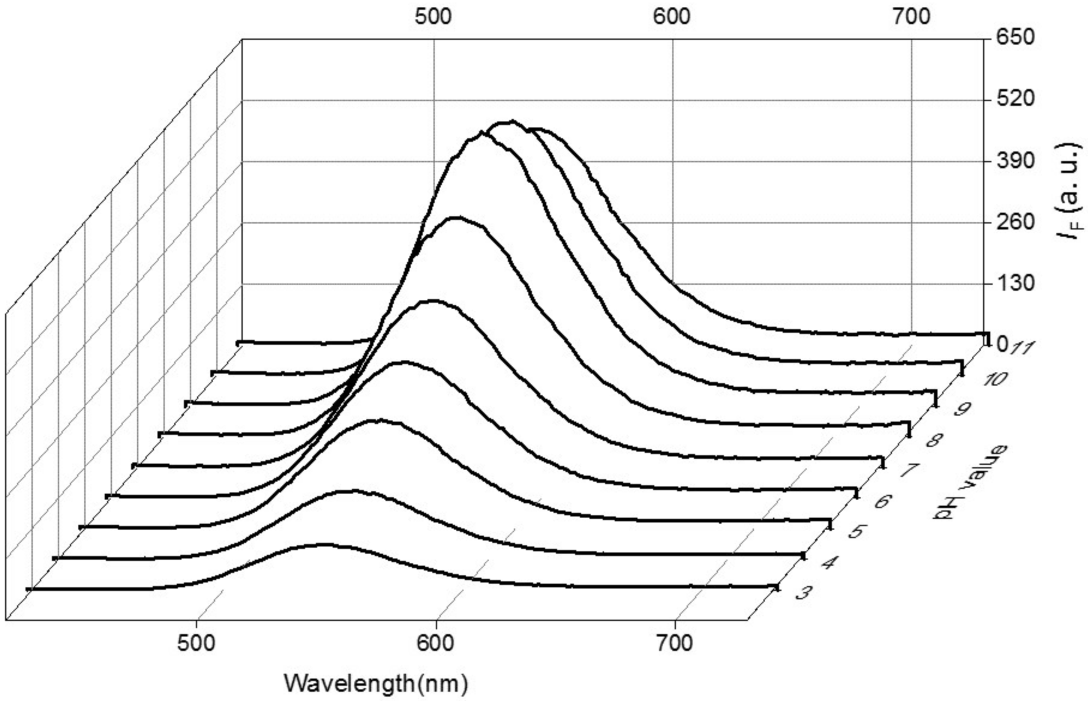

Fig. S11. PL emission spectra of 11-MUTAB–Au $NDs_{2.0h/20w}$ synthesized in different pH (3−11) sodium phosphate solution (20 mM). Excitation wavelength: 365 nm. Other conditions were the same as those described in Fig. 1.

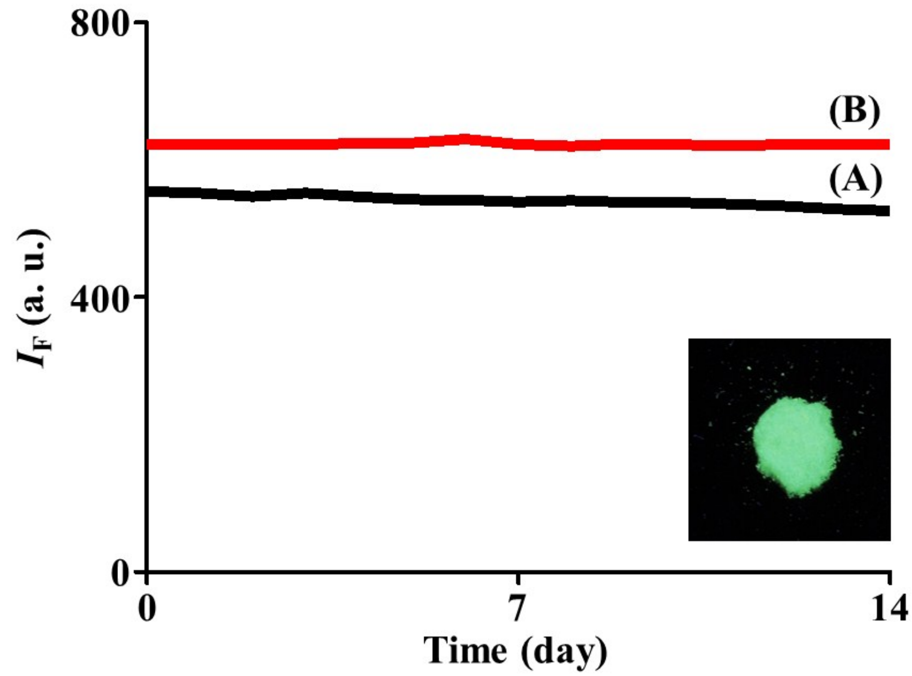

Fig. S12. Photoluminescence intensity of 11-MUTAB–Au $NDs_{2.0h/20w}$ in the (A) solution (prepared in 20 mM sodium tetraborate solution, pH 9.2) and (B) solid state recorded every day for 14 days. The 11-MUTAB–Au $NDs_{2.0h/20w}$ samples were stored at 4 °C in the dark. Inset: Photograph of the PL of the corresponding powder Au ND upon excitation (365 nm) under a hand-held UV lamp. Excitation wavelength: 365 nm. Other conditions were the same as those described in Fig. 1.

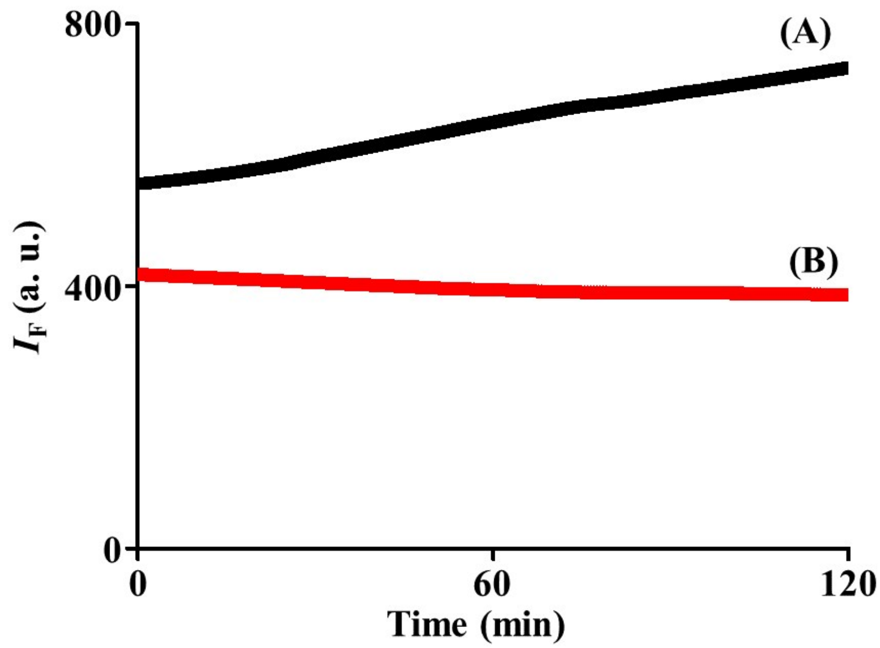

Fig. S13. Fluorescence intensity of (A) 11-MUTAB–Au NDs$_{2.0h/20w}$ (100 nM) and (B) 11-MUA–Au NDs (100 nM) in 20 mM sodium tetraborate solution (pH 9.2) during continuous excitation at 365-nm for 2 h.

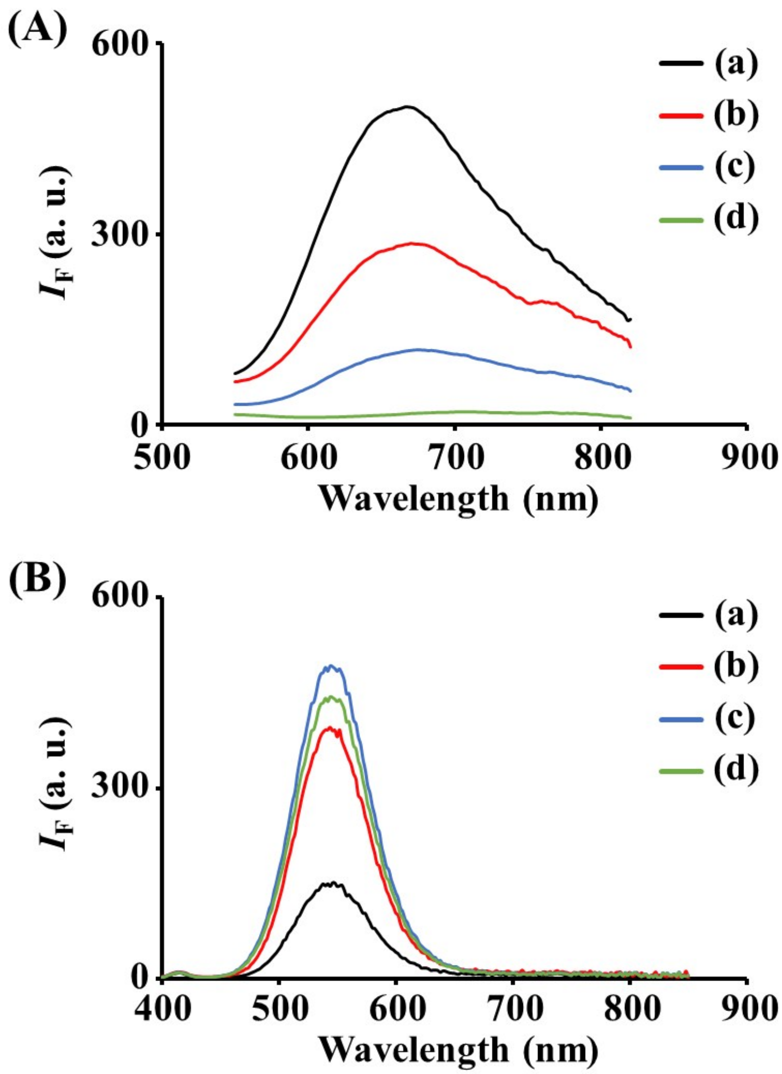

Fig. S14. (A) PL emission spectra of (a) 2-ME–Au NDs and (b–d) the sample in (a) after ultrasonication (20 W) for (b) 0.5, (c) 2.0, and (d) 5.0 h. (B) PL emission spectra of (a) 6-MH–Au NDs and (b–d) the sample in (a) after ultrasonication (20 W) for (b) 0.5, (c) 2.0, and (d) 5.0 h. Excitation wavelength: 365 nm. Other conditions were the same as those described in Fig. 1.

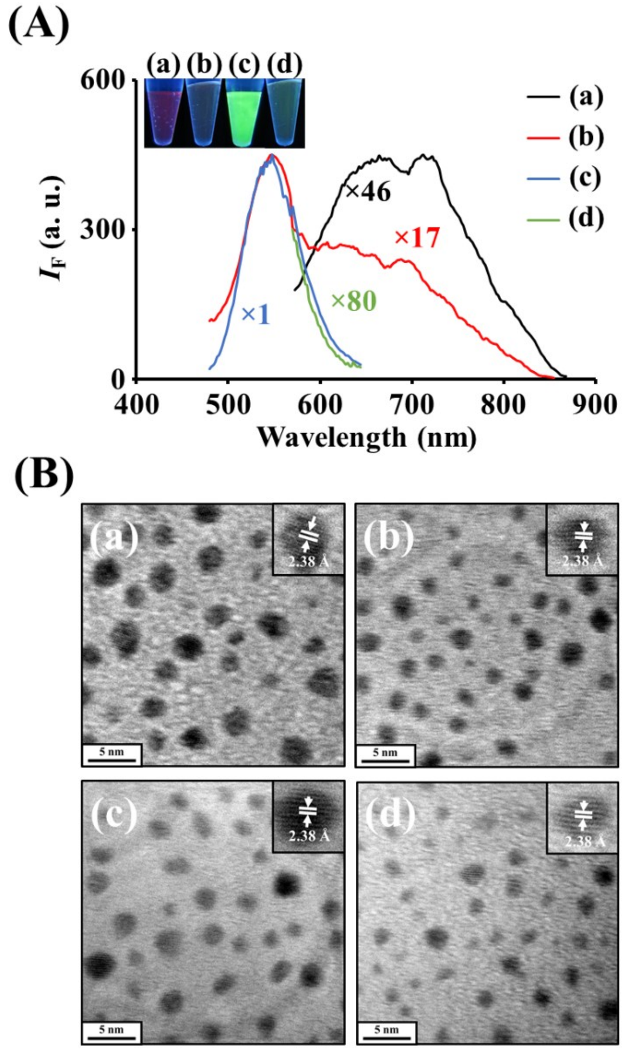

Fig. S15. (A) PL spectra and (B) TEM images of (a) 11-MUTAB–Au NDs and (b–d) the sample in (a) after ultrasonication (10 W) for (b) 0.5, (c) 2.0, and (d) 5.0 h. Excitation wavelength: 365 nm. The particle sizes of the samples in (a–d) (each calculated from 100 counts) were 1.75 ± 0.56, 1.64 ± 0.43, 1.60 ± 0.39, and 1.47 ± 0.46 nm, respectively. Other conditions were the same as those described in Fig. 1.

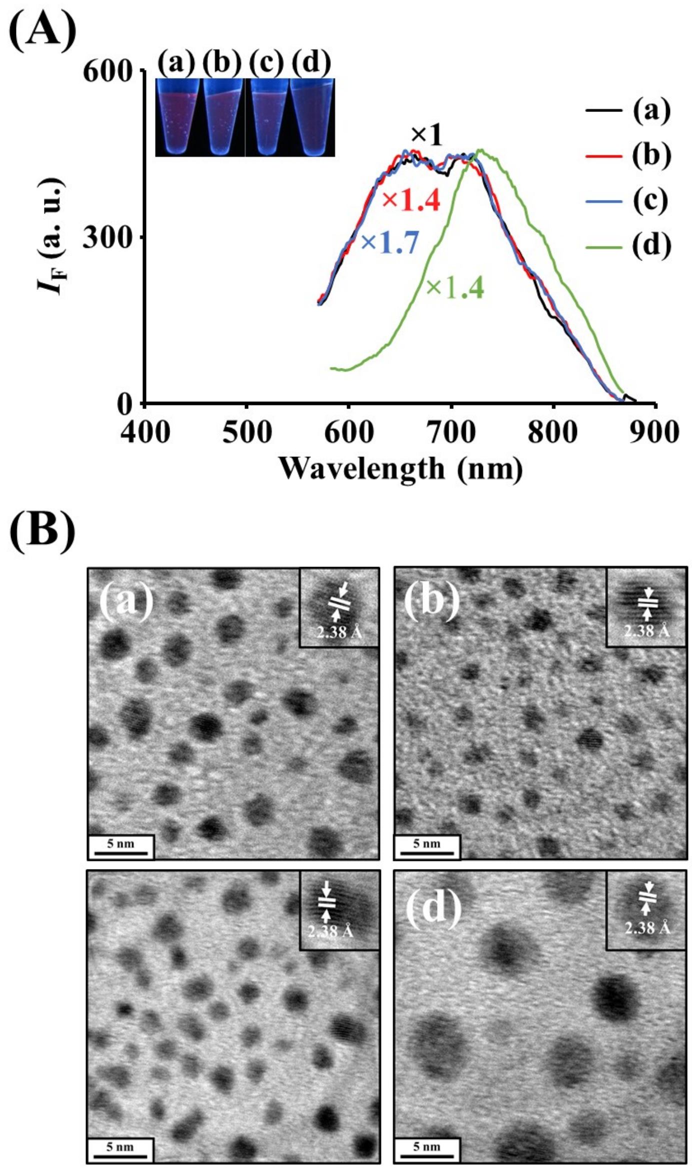

Fig. S16. (A) PL spectra and (B) TEM images of (a) 11-MUTAB–Au NDs and (b–d) the sample in (a) after ultrasonication (50 W) for (b) 0.5, (c) 2.0, and (d) 5.0 h. Excitation wavelength: 365 nm. The particle sizes of the samples in (a–d) (each calculated from 100 counts) were 1.75 ± 0.56, 1.71 ± 0.35, 1.72 ± 0.64, and 4.63 ± 0.40 nm, respectively. Other conditions were the same as those described in Fig. 1.